

Large-scale seismically guided anisotropic inversion of towed-streamer EM data in the Barents Sea

Michael S. Zhdanov^{1,2*}, Masashi Endo¹, Martin Čuma^{1,2}, David Sunwall¹, Jenny-Ann Malmberg³, Allan McKay³, Tashi Tshering³ and Jonathan Midgley³ present an anisotropic inversion technique for towed streamer EM data, which incorporates seismic constraints.

This paper presents a fast and efficient large-scale anisotropic inversion technique for towed streamer electromagnetic (EM) data, which incorporates seismic constraints. The inversion algorithm is based on the 3D contraction integral equation method and utilizes a re-weighted regularized conjugate gradient technique to minimize the objective functional (Zhdanov et al. 2014a, b). We have also introduced the concept of a moving sensitivity domain for seismically guided EM inversion, originally developed for airborne EM surveys (Zhdanov and Cox, 2013), which makes it possible to invert the entire large-scale towed streamer EM survey data while keeping the accuracy of the computation of the EM fields. The developed algorithm and software can take into account the constraints based on seis-

mic and well-log data, and provide the inversion guided by these constraints.

To demonstrate the practical effectiveness of this approach for large-scale inversion of marine EM data, as well as integration with seismic data, we apply the method to the inversion of about 2000 line-km of towed streamer EM data. The data form part of a larger survey in the Norwegian Barents Sea (McKay et al., 2016). We show that the technique produces a single resistivity model that is consistent with both the measured EM data and the main seismically defined structures. Thus, the resistivity model is ready to be interpreted and used in further quantitative interpretation studies.

Geological setting of the survey area

The Barents Sea was formed by two major continental collisions and subsequent separation. The first event was the Caledonian orogeny, some 400 Ma. The Caledonian fold belt runs N-S through Scandinavia and the Svalbard Archipelago and mainly influences the western part of the Barents Sea. The second collision event was the Uralian orogeny, about 240 Ma. Running from East Russia up along Novaya Zemlya, the Uralian fold belt has caused an N-S structural grain in the rocks of the eastern Barents Sea (Doré, 1994).

The most significant proportion of the HC reserves proven to date in both the Norwegian and Russian Barents Sea is contained within the strata of the Jurassic age. The major discoveries in the Norwegian sector – Snøhvit, Albatross and Askeladden – all share a principal reservoir consisting of Lower-Middle Jurassic sandstone. This unit was deposited in a coastal marine setting and, where penetrated in the Hammerfest Basin, usually had very favourable reservoir properties (high porosity and permeability). Larsen et al. (1993) have estimated that about 85% of the Norwegian Barents Sea HC resources lie within this formation. The traps that form the Norwegian Jurassic fields are generally

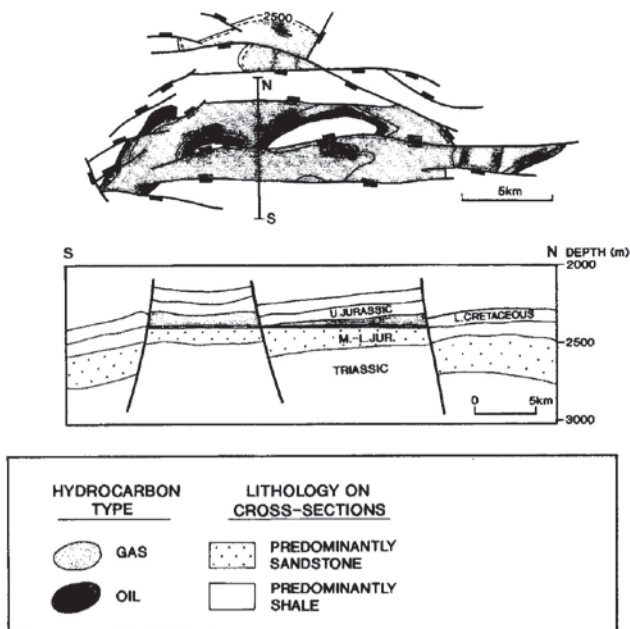


Figure 1 Sketch map and geological cross-section of the Snøhvit Field (after Doré, 1994).

¹ TechnoImaging.

² Consortium for Electromagnetic Modeling and Inversion (CEMI).

³ PGS.

* Corresponding author, E-mail: mzhdanov@technoimaging.com

Marine Seismic

fault-bounded positive blocks, and the HC are sealed by overlying Upper Jurassic shales (Doré, 1994; Figure 1).

Towed streamer EM survey in the Barents Sea

More than 10,000 line-km of EM data were acquired in the Barents Sea in 2014 by the current generation of the towed-streamer EM system (Engelmark et al., 2014). The towed-streamer EM survey was conducted using an 800-m long bipole electric current source with 1500 Amperes current towed at a depth of 10 m, and a streamer cable which measured in-line electric fields with offsets from 0 to 7733 m in a frequency range from 0.2 to 9.8 Hz at a depth of 100 m from the sea surface.

In the current case study, we used a total of 2167 line-km of the towed streamer EM data covering the survey area of ~1500 km² (Figure 2) with offsets from 1888 to 7733 m in a frequency range from 0.2 to 3.0 Hz.

Inversion methodology and workflow

3D inversion of towed streamer EM data is a very challenging problem because of the huge number of transmitter positions of the moving towed-streamer EM system, and, correspondingly, the huge number of 3D forward and inverse problems that need to be solved for every transmitter position over the large survey area. We overcame this problem by using the moving sensitivity domain approach (Zhdanov et al., 2014a, b). This approach exploits the fact that the towed-streamer EM system's sensitivity domain is significantly less than the size of the survey area, and we introduce the concept of 3D inversion with a moving sensitivity domain (MSD). That is, for a given transmitter-receiver pair, the responses and Fréchet derivatives (data sensitivities) are computed from a 3D earth model that encapsulates the towed EM system's sensitivity. The MSD technique, critical for this large-scale problem, requires the assembling of a global sensitivity matrix for the entire inversion domain, corresponding to the total survey area. The code runs a simultaneous inversion of the full survey,

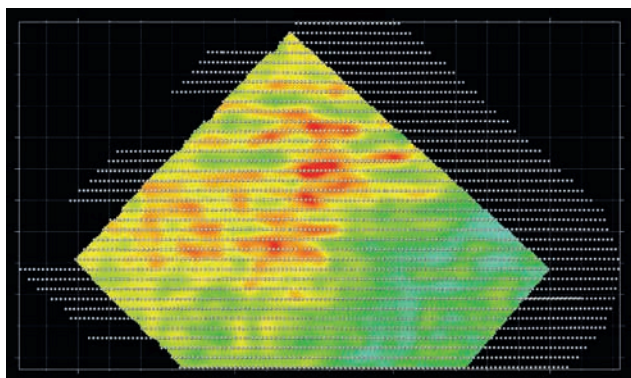


Figure 2 A shot-point map of the towed-streamer EM survey in the Barents Sea and a depth slice at -700 m of the horizontal resistivity of the guided inversion. The shot interval is 250 m and the line spacing is 1.25 km.

but since the sensitivity matrix becomes sparse owing to the MSD approach, the memory requirements are reduced dramatically and make large-scale inversion feasible. The 3D forward modelling is based on the rigorous integral equation (IE) method, and the inversion problem is solved using the regularized conjugate gradient (RCG) algorithm with adaptive regularization. The code is fully parallelized over a PC cluster to run large-scale 3D inversion.

There are several important components/steps of the developed inversion method:

1. 1D inversions of the towed-streamer EM data:
 - a. Determination of a general (variable) background geoelectrical model.
2. 3D unconstrained inversion of the towed-streamer EM data:
 - a. Construction of the a priori model (variable background) based on 1D inversion results and known information, such as bathymetry and seawater conductivity.
 - b. 3D unconstrained inversion with variable background.
3. 3D guided inversion of the towed-streamer EM data:
 - a. Construction of the a priori model based on 3D unconstrained inversion results and seismic data (seismic horizons).
 - b. 3D guided inversion with the constructed a priori model.

Note that, even in the case of 3D guided inversion, all resistivity values in the inversion domain are still free to change to minimize the parametric functional (a combination of the misfit and stabilizing functionals (Zhdanov, 2015)). In other words, the a priori model only guides the solution towards a more geologically plausible model, while maintaining a similar level of the misfit between the observed and predicted data (Zhdanov et al., 2014a, 2014b, 2015).

Figure 3 shows vertical cross sections of the 3D a priori model used for 3D guided inversion along $Y = 100$ m. The seismic horizons are shown as dashed lines in this figure. Note that, the resistivity values in the volume between the seismic horizons in the a priori model are specified by averaging the resistivity values recovered from 3D unconstrained inversion within the same volume.

Inversion results

The dimensions of the inversion domain were selected as follows: 84 km in the x direction (parallel to the survey lines); 44 km in the y direction (perpendicular to the survey lines); 3 km in the z direction. This rectangular region was discretized into cells of 50 m x 50 m in the horizontal directions, and from 12.5 m to 200 m (43 layers total) in the vertical direction. The selected towed-streamer EM data for the inversion consisted of a total of 594,125 data points with 24 offsets (approximately from 1900 m to 7700 m) and seven frequencies (from 0.2 Hz to 3.0 Hz) along 37 survey lines (Figure 2). It took

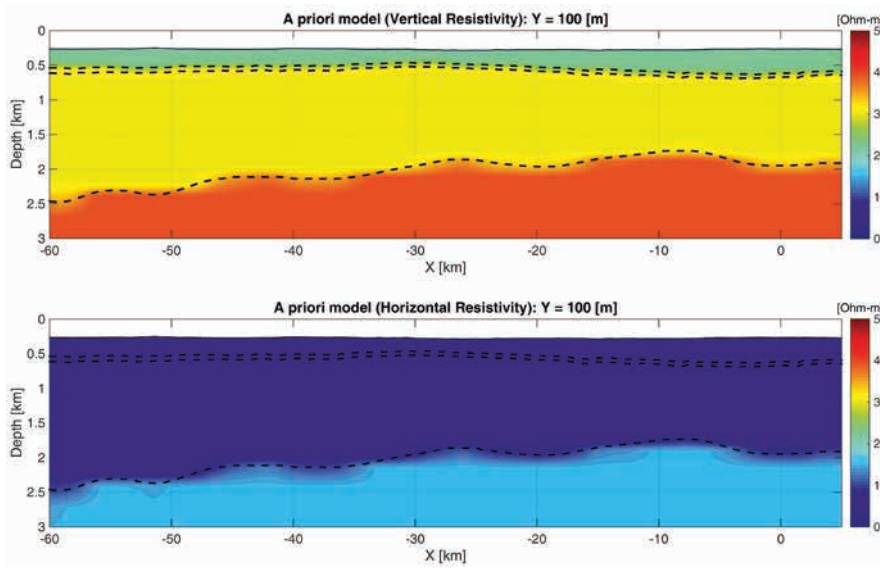


Figure 3 Vertical cross sections of the 3D a priori model (top panel shows the vertical resistivity; bottom panel presents the horizontal resistivity) with seismic horizons (dashed lines) used for 3D guided inversion along $Y = 100$ m.

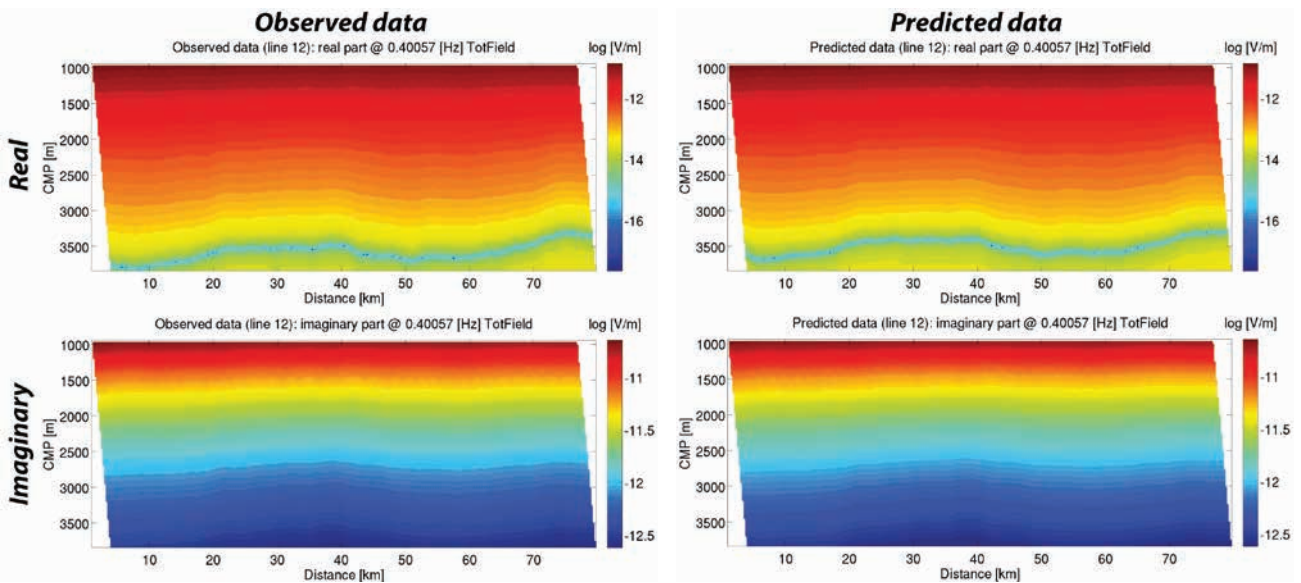


Figure 4 CMP plots of the observed (left panels) and predicted (right panels) EM data (top panels; show the real parts of the observed data, bottom panels present the imaginary parts) along line 12.

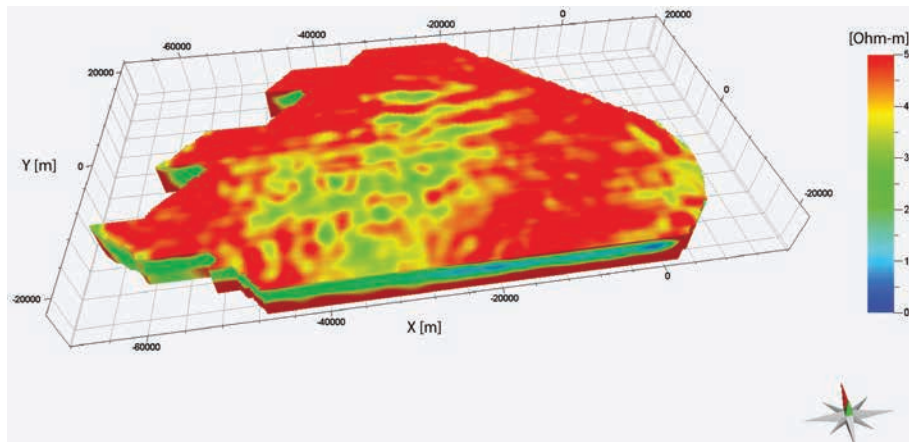


Figure 5 A 3D view of 3D vertical resistivity model recovered from 3D inversion. The top of the 3D volume corresponds to 700 m below the sea level.

Marine Seismic

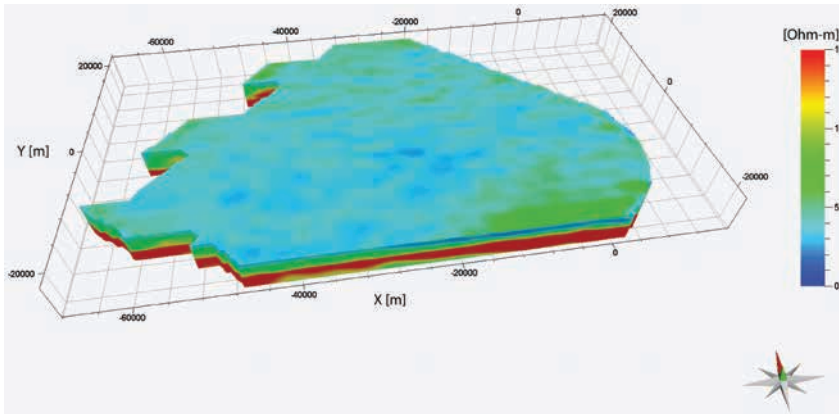
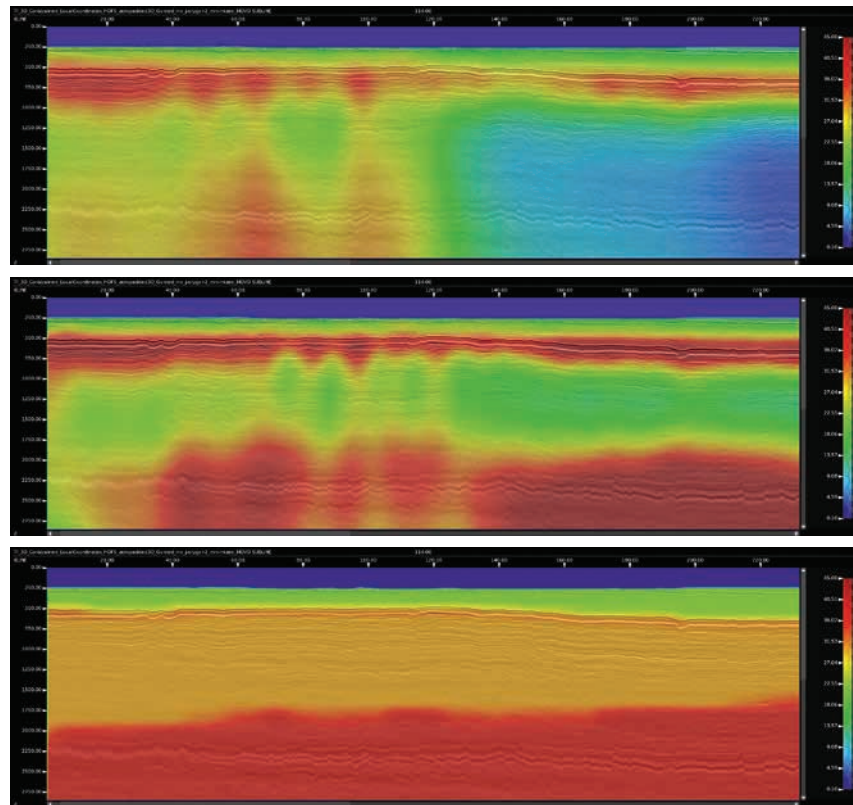


Figure 6 A 3D view of 3D horizontal resistivity model recovered from 3D inversion. The top of the 3D volume corresponds to 700 m below the sea level.

Figure 7 Vertical cross sections of the 3D vertical resistivity (0.1-45 Ω m) recovered from 3D unconstrained (top panel) and guided (middle panel) inversion along a survey line overlain with 3D seismic data. The corresponding a priori model used for the guided inversion is shown in the bottom panel.



about 60 hours to run this large-scale 3D inversion on the PC cluster with 128 cores. Figure 4 shows examples of the CMP plots of the observed and predicted EM data along line 12. One can see a good agreement between the observed and predicted data, and the final misfit (the L2 norm of the difference between the observed and predicted data normalized by the L2 norm of the observed data) converged to 2.4 %.

Figures 5 and 6 represent 3D views of the 3D vertical and horizontal resistivity models recovered from 3D guided inversion. The top of the 3D volume in these figures corresponds to 700 m below the sea level.

Figure 7 shows an example of the vertical cross section of the 3D anisotropic geoelectrical model (vertical

resistivity) recovered from 3D unconstrained (top panel), and guided inversion (middle panel), overlain with 3D seismic data. The corresponding a priori model used for the guided inversion is shown in the bottom panel. In general, a slight change in the resistivity model can be observed when running guided-compared to unconstrained inversion, resulting in a tighter inversion result and more well-defined structures.

Figure 8 shows an example of the vertical cross section of the square of the anisotropic coefficient, λ , recovered from 3D unconstrained (top panel) and guided (middle panel) inversion along a survey line with 3D seismic data overlain. The corresponding a priori model is shown in the

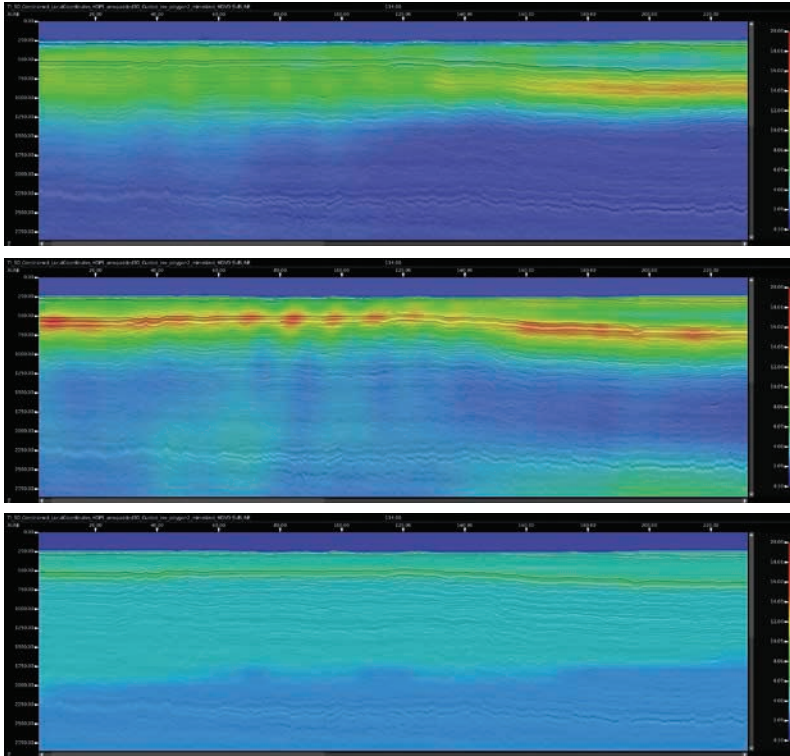


Figure 8 Vertical cross sections of the square of the 3D anisotropic coefficient model (0.1-20) recovered from 3D unconstrained (top panel) and guided (middle panel) inversion along a survey line overlain with seismic data. The corresponding a priori model used for the guided inversion is shown in the bottom panel.

bottom panel. The anisotropic coefficient was calculated as follows:

$$\lambda = \sqrt{\frac{\rho_v}{\rho_h}},$$

where ρ_v and ρ_h are vertical and horizontal resistivities, respectively. In the case of the guided inversion, anisotropic structures appear more clearly than in the unconstrained inversion.

Conclusions

We have developed an approach to incorporate seismic constraints in the 3D EM inversion algorithm, based on the 3D contraction integral equation method and the concept of a moving sensitivity domain. The seismically guided anisotropic inversion of the large-scale towed streamer EM survey, acquired over the Barents Sea, produced features that agreed well with the general geological structures in the survey area and other available geophysical information. By using this method, an uplift in the resistivity model could be observed compared to running unconstrained inversion. The new method of seismically guided EM inversion has been proven to be efficient for a large towed-streamer EM dataset in a complex geological setting.

Acknowledgements

We would like to thank PGS for the right to present the results of this towed-streamer EM survey and TechnoImaging for its support of the research and permission to publish.

References

- Doré, A.G. [1994]. Barents geology, petroleum resources and commercial potential. *Arctic Institute of North America*, 48, 207-221.
- Engelmark, F., Mattsson, J., McKay, A. and Du, Z. [2014]. Towed streamer EM comes of age. *First Break*, 32 (4), 75-78.
- Larsen, R.M., Fjæran, T. and Skarpnes, O. [1993]. *Hydrocarbon potential of the Norwegian Barents Sea based on recent well results*. In: Vorren et al., (Eds.) Arctic geology and petroleum potential, NPF Special Publication 2, 321-331.
- McKay, A., Ronholt, G., Tshering, T. and Naumann, S. [2016]. Joint interpretation of high-resolution velocity and resistivity models from the Barents Sea. *First Break*, 34 (4), 73-77.
- Zhdanov, M.S. and Cox, L. [2013]. *Method of subsurface imaging using superposition of sensor sensitivities from geophysical data acquisition systems*. U. S. Patent US 2013/0173163.
- Zhdanov, M.S., Endo, M., Cox, L.H., Cuma, M., Linfoot, J., Anderson, C., Black, N. and Gribenko, A.V. [2014a]. Three-dimensional inversion of towed streamer electromagnetic data. *Geophysical Prospecting*, 62, 552-572.
- Zhdanov, M.S., Endo, M., Yoon, D., Mattsson, J. and Midgley, J. [2014b]. Anisotropic 3D inversion of towed streamer EM data: Case study from the Troll West Oil Province. *Interpretation*, 2, SH97-SH113.
- Zhdanov, M.S., Endo, M., Sunwall, D. and Mattsson, J. [2015]. Advanced 3D imaging of complex geolectrical structures using towed streamer EM data over the Mariner field in the North Sea. *First Break*, 33, 59-63.
- Zhdanov, M.S. [2015]. *Inverse theory and applications in geophysics*. Elsevier.